Electronic Supplementary Material (ESI) for Lab on a Chip.

Supporting Information

Customizable single-layer hydrogel robot with programmable NIR-triggered responsiveness

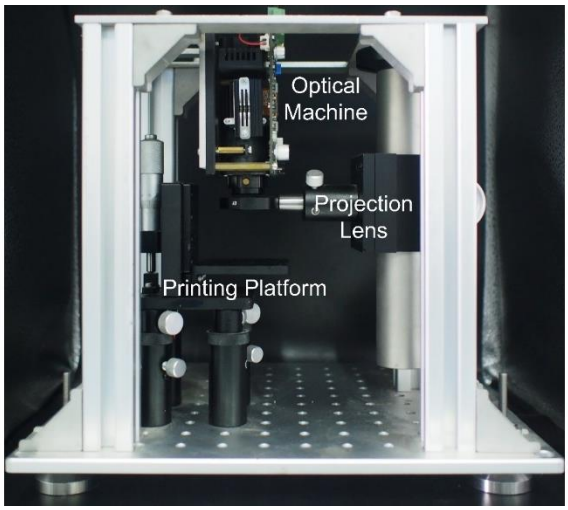

Figure S1. High Presision Digital Light Processing 3D printing system.

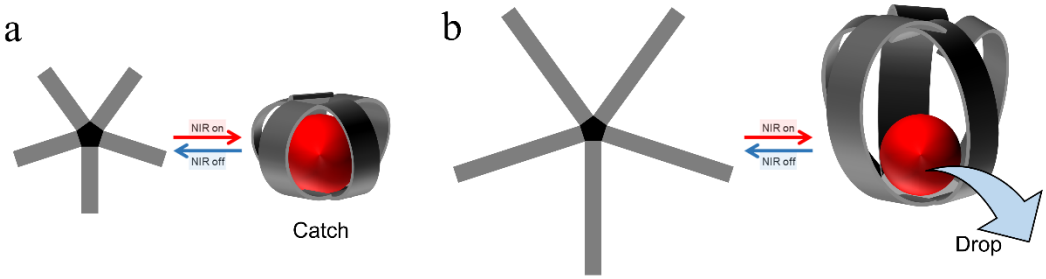

Figure S2. Morphological differences between hydrogel robots with L/W = 4 and L/W = 8.

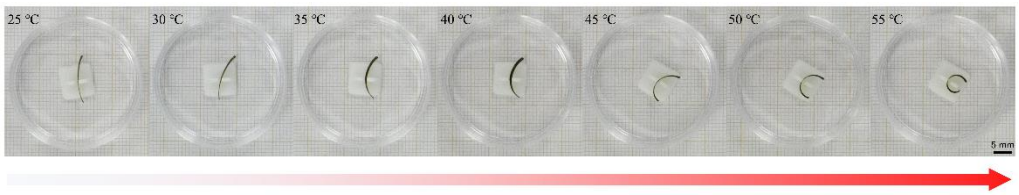

Figure S3. Response process of hydrogel robot with temperature.

Magnetron characterization and applications

The energy dispersion spectral mapping image shown in Figure S3a shows the partial morphological structure of a hydrogel robot obtained using secondary electrons and the distribution of three elements (C, N and Fe). N and Fe coexist uniformly in hydrogel robot. The results show that PDA and MNPs are evenly loaded onto the surface of the hydrogel robot. Here, VSM experiments were performed to obtain the magnetic properties of hydrogel robot and pure Fe_3O_4 magnetic nanoparticles, where hysteresis cycles were between -15 and +15 KOe at 25 ℃. The magnetization curves of the fabricated hydrogel robot and pure Fe_3O_4 magnetic nanoparticles are shown in Figure S3b. The coercivity and magnetic saturation of Fe_3O_4 and robot are 726.8 Oe and 53.33 emu/g and 1106.3 Oe and 9.76 emu/g, respectively. The coercivity and magnetic saturation values of the hydrogel robot are smaller than those of pure Fe_3O_4 magnetic nanoparticles, because the magnetic nanoparticles content of the hydrogel robot is low, and the hydrogel robot is composed of magnetic and non-magnetic materials (composite 3D printing ink). X-ray diffraction (XRD) analysis was conducted on the prepared single-layer hydrogel robot and the hydrogel robot with MNPs added, and the results are shown in Figure S3c. A series of different peaks were observed for each sample in the 2θ region ranging from 30° to 80°.

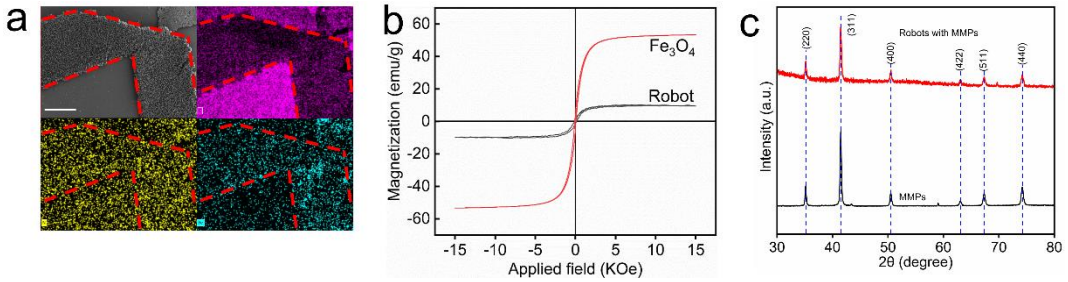

Figure S4. Characterization of hydrogel machine robots with added MMPs. **(a)** Scanning electron microscopy (SEM) and energy dispersive X-ray spectroscopy (EDS) images of the robot's partial structure. (Scale bar: 600 μm). **(b)** Vibrating sample magnetometer (VSM) measurements of MNPs (red) and hydrogel robot (black). **(c)** X-ray diffraction (XRD) measurements of MNPs (red) and hydrogel robot (black).

Here, we demonstrate the delivery and release of 3D-printed cargo via NIR light on and off stimuli using a hydrogel robot with magnetic nanoparticles added. First, PBS buffer solution was added to the channel to simulate the humoral environment. Figure S4,5 and Video S8,9 show the transport and release of the target over time. Initially, we turned on the NIR and placed the robot, which was already wrapped in the target, under the area called the starting point; The tumbling or translation motion generated by the magnet drives the robot to the target area. At this time, we turn off the NIR, and the robot unbend, resulting the cargo release. Finally, drive by the magnet to recover the robot.

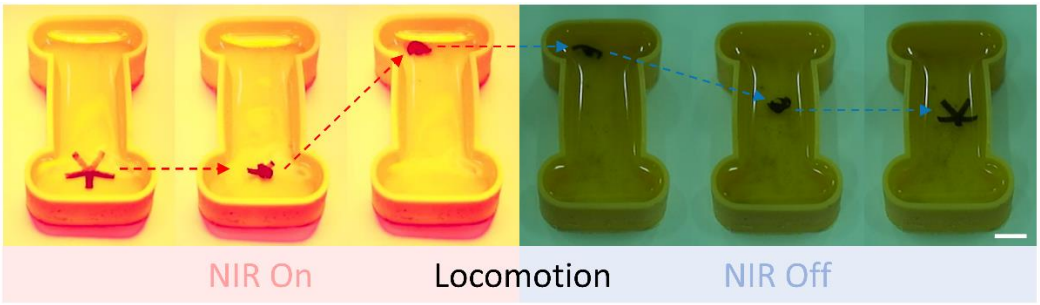

Figure S5. NIR-triggered Responsiveness and magnetically guided process. (Scale bar: 1 cm).

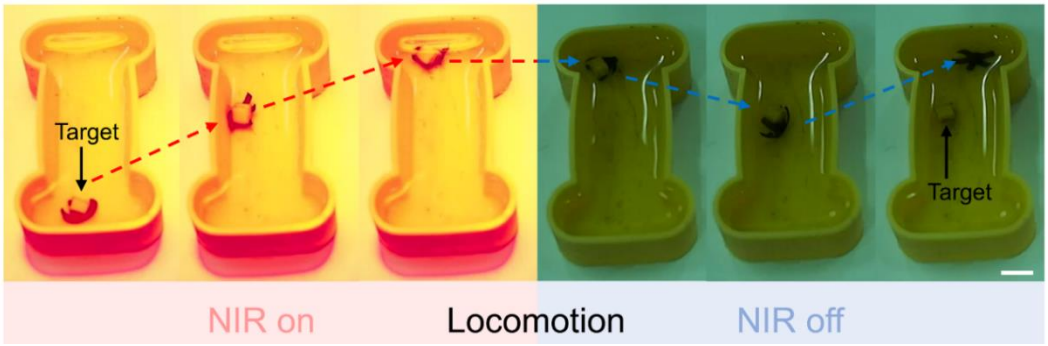

Figure S6. The hydrogel robot simulates the cargo delivery and recovery. (Scale bar: 1 cm).

Biocompatibility testing

To evaluate the biocompatibility of hydrogel robot, we co-cultured 293T cells with the hydrogel robot and stained the cells with Calcein AM/PI (Figure S6). After 24 h, 48 h and 72 h of co-culture (green cells were viable cells and red cells were dead cells). With cell proliferation, the survival rate of cell was 93.09%, 96.74% and 95.31%, respectively. The results show that the hydrogel robot has good biocompatibility and can extend the biomedical applications of 3D printed multi-responsive smart hydrogel.

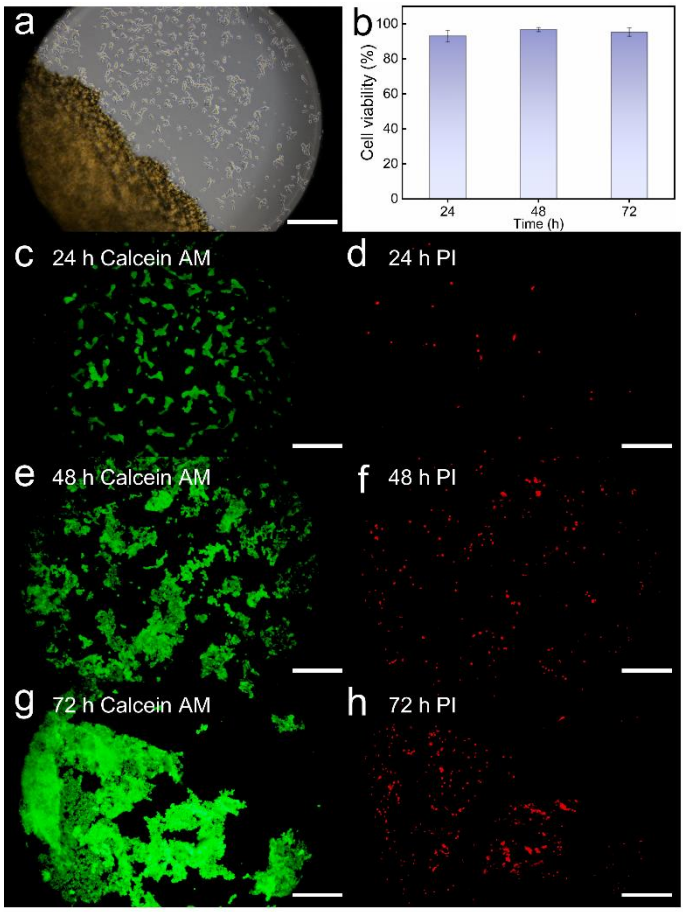

Figure S7. Biocompatibility testing of hydrogel robot. **(a)** Photographs of cell and hydrogel robot co-culture. **(b)** Viability of 293T cells co-cultured with hydrogel for 72 h. **(c-h)** Calcein AM/ PI cell staining on 24 h, 48 h and 72 h. (Scale bar: 400 μm).

Supplementary Videos

Video S1. The response process of robot arm under NIR light.

Video S2. Deformation and recovery process of four-arm robot.

Video S3. Deformation and recovery process of five-arm robot.

Video S4. Deformation and recovery process of six-arm robot.

Video S5. The wrapping process of the hand-shaped hydrogel robot.

Video S6. The three-arm robot performs a response sequence based on the photon intensity.

Video S7. The four-arm robot performs a response sequence based on the photon intensity.

Video S8. NIR-triggered Responsiveness and magnetically guided process.

Video S9. The hydrogel robot simulates the cargo delivery and recovery.